

# Journal of Materials Chemistry C

Accepted Manuscript



This is an *Accepted Manuscript*, which has been through the Royal Society of Chemistry peer review process and has been accepted for publication.

*Accepted Manuscripts* are published online shortly after acceptance, before technical editing, formatting and proof reading. Using this free service, authors can make their results available to the community, in citable form, before we publish the edited article. We will replace this *Accepted Manuscript* with the edited and formatted *Advance Article* as soon as it is available.

You can find more information about *Accepted Manuscripts* in the [Information for Authors](#).

Please note that technical editing may introduce minor changes to the text and/or graphics, which may alter content. The journal's standard [Terms & Conditions](#) and the [Ethical guidelines](#) still apply. In no event shall the Royal Society of Chemistry be held responsible for any errors or omissions in this *Accepted Manuscript* or any consequences arising from the use of any information it contains.

Submitted to *Journal of Materials Chemistry C*

**Polyoxometalate-based Organic-Inorganic Hybrids for  
Stabilization and Optical Switching of Liquid Crystal Blue  
Phase**

Jiao Wang,<sup>1‡</sup> Chang-Gen Lin,<sup>2‡</sup> Junyan Zhang<sup>1</sup>, Jie Wei<sup>1</sup>, Yu-Fei Song,<sup>2\*</sup> Jinbao Guo<sup>1\*</sup>

<sup>1</sup>College of Materials Science and Engineering, Beijing University of Chemical Technology, Beijing 100029, P. R. China.

<sup>2</sup>State Key Laboratory of Chemical Resource Engineering, Beijing University of Chemical Technology, Beijing 100029, P. R. China.

<sup>‡</sup>These authors contributed equally to this work.

Corresponding authors: [guojb@mail.buct.edu.cn](mailto:guojb@mail.buct.edu.cn)

[songyf@mail.buct.edu.cn](mailto:songyf@mail.buct.edu.cn)

**Abstract:**

We develop two novel bent- and dendritic-like polyoxometalate (POM) organic-inorganic hybrids with covalently grafted azobenzene mesogenic moieties for stabilization and optical switching of BPs. The bent-like POMs hybrid is found to be great effective for the stabilization of BP I, in which the widest BP I temperature ranges could reach to 20.5 °C. Moreover, what surprises us is that, dendritic-like POMs hybrid could help to stabilize BP II. The related physical mechanisms of the BPs stabilization are discussed on the basis of elastic characteristics and orientational order of LC molecules. Additionally, the wide optical tuning of Bragg reflection band of BP II is demonstrated, in which the shift of Bragg reflection wavelength is around 80 nm. This work opens up a new way for developing the BP systems that exhibit wide temperature ranges and good switching effect by optical fields, leading to the potential applications in display fields as well as optoelectronic devices.

## 1. Introduction

Liquid crystals (LCs) represent a vast and diverse class of anisotropic soft matter materials. They exist as various phases that are stable at different temperature ranges.<sup>1,2</sup> Among the various LC phases, blue phases (BPs) with three-dimensional superstructures have attracted much attention due to their potential for the application in optical and display fields and also their analogous topological structures in condensed matter systems.<sup>3-7</sup> In general, BPs could be observed in cholesteric LCs (Ch-LCs) with strong chirality strength on the cooling process from the isotropic state. According to spatial orientation, BPs could be classified into three thermodynamically distinct phases (BP I, BP II and BP III). BP I has body-centered cubic structure and BP II has simple cubic structure, while BP III is amorphous with a local cubic lattice structure.<sup>8-11</sup>

Practical BP devices remain elusive for decades despite their promising efficient LC display and emergent photonic applications. The formation of BP I and BP II could be considered as a stack of double twist cylinders (DTC), in which neighboring LC molecules twist slightly to each other to constitute a helicoidal twist. However, molecular orientations cannot extend smoothly in the space between the cylinders, thereby forming a network of disclinations. The places of disclinations are associated with high energy, which are most disfavored regions in BPs. As a result, the thermal stability of BPs is limited to only one or two degrees near the isotropic clearing point due to the high free energies of the disclination lines.<sup>6</sup> Therefore, many efforts have been paid to solve this challenge by employing polymer networks, nanoparticles and special molecular design using T-shaped molecules, dimer molecules and bent-core molecules.<sup>12-32</sup> Meanwhile, there has been continuing interest in the development of smart BP materials which

respond to external stimuli, such as electrical field, temperature and optical field. Among external stimuli methods, optically switchable BPs behavior can be efficiently achieved based on *trans-cis* photoisomerization of azobenzene.<sup>20,33-35</sup>

In this work, we develop two novel bent- and dendritic-like POMs organic-inorganic hybrids containing azobenzene mesogenic ligands to stabilize the BPs as well as to optically switch Bragg reflection band of BPs. As is well known, polyoxometalates (POMs) stand for a family of discrete anionic metal oxides constituted by transition metals such as V, Mo, W, *etc.* in their highest oxidation states. The intriguing physical and chemical properties of POMs render them capable candidates for the development of multifunctional materials ranging from 3D printer, catalysis, electron transfer, anticorrosion to soft mater *etc.*<sup>36-44</sup> Furthermore, one of the most attractive aspects of POMs is the fact that these nano-sized clusters can be used as transferable building blocks to form organic-inorganic hybrid assemblies by tethering functional organic components onto POMs.<sup>45,46</sup> Herein, we focus on the effect of molecule structure of POMs hybrids on the phase behaviors of BPs. Interestingly, we find that bent-like POMs hybrid has a great effect for the stabilization of the BP I; while dendritic-like POMs hybrid has a positive influence for stabilizing the BP II. The corresponding physical mechanisms of the stabilization effect on BPs are investigated in detail. Finally, the wide optical switching of Bragg reflection band of BP II based on the *trans-cis* photoisomerization of azobenzene ligand in dendritic-like POMs hybrid is demonstrated.

## 2. Experimental Sections

### 2.1 Materials

Nematic LCs, BYLC-X ( $\Delta n=0.20$  at 589 nm wavelength and 20°C; Beijing Bayi Space

LCD Technology CO., LTD.); S811 (chiral dopant, Beijing Lyra Tech). POM Hybrid 1 and POM Hybrid 2 were synthesized for the use of study. The chemical structures of POM Hybrid 1 and 2 are shown in **Figure 1**. The detailed synthetic procedures and characterizations of them are provided in electric supporting information (ESI).

## 2.2 LC sample preparation

In order to measure optical performance of BPs, LC cells were made from two pieces of glass bonded together and no surface alignment layer were used, and polyethylene terephthalate (PET) film of 12  $\mu\text{m}$  thickness was used as the cell spacers. The LC mixture was filled into the cell at an isotropic state, and cooled down to BP temperature at a rate of 0.5  $^{\circ}\text{C}/\text{min}$ . Then the LC cell was kept for the purpose of testing and optical switching.

## 2.3 Measurements

The optical textures of the LC samples were observed using a polarized light microscope (Leica, DM2500P) with a heating stage of an accuracy of  $\pm 0.1$   $^{\circ}\text{C}$  (LTS 420), and the optical images were recorded using Linksys 2.43 software. The Bragg reflection wavelength of BPs were obtained by fiber spectrometer (Avantes, AvaSpec-2048), and the sample temperatures were precisely controlled by the hot stage of LTS 420. For the measurement of elastic constants, the LC sample was filled into a glass-sandwiched cell with ITO electrode, in which the cell gap of  $d$  was 22.02  $\mu\text{m}$  and a polyimide thin film was coated on the glass substrate as a homogeneous alignment layer. The electric fields were applied in the direction perpendicular to the substrate surface. A threshold voltage ( $V_{\text{th}}$ ) and dielectric constant anisotropy ( $\Delta\epsilon$ ) were obtained with capacitance method by employing a capacitance–voltage ( $C$ – $V$ ) measurement system (INSTECH ALCT-PP1). Here the temperatures of LC samples were controlled by an accurate temperature control

stage (INTEC mk1000). The detailed measurement and calculation processes were very similar to the previous study,<sup>14</sup> and the related parameters are listed in ESI.

### 3. Results and Discussion

#### 3.1. Design Strategy and Synthesis of POM hybrids

To achieve the POM hybrids, photo-responsive azobenzene mesogenic units are covalently grafted onto the nanosized POM clusters. As shown in **Figure 1**, we design two organic-inorganic hybrids with the general molecular formulas of  $(\text{TBA})_4[(\text{SiW}_{11}\text{O}_{39})\text{O}\{\text{Si}(\text{CH}_2)_3\text{NHCOC}_6\text{H}_4\text{N}=\text{NC}_6\text{H}_4\text{OC}_8\text{H}_{17}\}_2]$  (POM Hybrid 1 with a bent-like structure),  $\text{TBA}=(n\text{-C}_4\text{H}_9)_4\text{N}^+$  (counter cation for the charge balancing) and  $(\text{TBA})_4[(\text{SiW}_{11}\text{O}_{39})\text{O}\{\text{SiCH}_2)_3\text{NHCOC}_6\text{H}_3[\text{O}(\text{CH}_2)_{12}\text{OC}_6\text{H}_4\text{N}=\text{NC}_6\text{H}_4\text{OC}_8\text{H}_{17}]_2]$  (POM Hybrid 2 with dendritic-like structure). The detailed description for synthetic processes and characterizations are provided in ESI as mentioned above. In brief, the POM hybrids were prepared by covalently attaching azobenzene mesogenic units onto  $[(\text{C}_4\text{H}_9)_4\text{N}]_4[(\text{SiW}_{11}\text{O}_{39})\text{O}\{\text{Si}(\text{CH}_2)_3\text{NH}_2\cdot\text{HCl}\}_2]$  (**SiW<sub>11</sub>-NH<sub>2</sub>**) Keggin POM cluster as similar to the previous studies.<sup>45,46</sup> As a representative case, the synthetic procedure of POM Hybrid 2 is provided in **Figure 2**. Various techniques including NMR, FT-IR, ESI-MS and elemental analyses are adopted to characterize the structural conformations of POM Hybrids 1 and 2. In the FT-IR spectra, C=O ( $1650\text{ cm}^{-1}$ ), Si-O-Si ( $1045\text{ cm}^{-1}$ ), W=O ( $960\text{ cm}^{-1}$ ) and W-O-W ( $850\text{ cm}^{-1}$ ) stretching vibrations can be clearly observed, indicating the organic motifs have been successfully anchored onto the POMs. <sup>1</sup>H-NMR spectra of POM Hybrids 1 and 2 show signals that can be assigned unambiguously and fit well with the corresponding molecular structures (see **Figure S1** and **Figure S2** in ESI). The peaks observed at ca. -52 ppm and -85 ppm in the <sup>29</sup>Si-NMR spectra of POM

Hybrids 1 and 2 correspond to the Si in the silane and the heteroatom of the  $\text{SiW}_{11}\text{O}_{40}$  cluster, respectively. ESI-MS provides convincing conformational information of POM Hybrids 1 and 2, and it is possible to assign all the signals (see **Figure S3-S4** and **Table S1 and S2** in ESI). For example, ESI-MS peaks of POM Hybrid 1 observed at  $m/z$  2044.52 can be ascribed to  $\{\text{HCOONa}+(\text{TBA})_2[(\text{SiW}_{11}\text{O}_{40})\{\text{Si}(\text{CH}_2)_3\text{NHCOC}_6\text{H}_4\text{N}_2\text{C}_6\text{H}_4\text{OC}_8\text{H}_{17}\}_2]\}^{2-}$  (**Figure 1**), while peaks of POM Hybrid 2 at  $m/z$  2794.97 can be assigned to  $\{(\text{TBA})_2[(\text{SiW}_{11}\text{O}_{40})\{\text{Si}(\text{CH}_2)_3\text{NHCOC}_6\text{H}_3-(\text{O}(\text{CH}_2)_{12}\text{OC}_{12}\text{H}_8\text{N}_2\text{OC}_8\text{H}_{17})_2\}_2]\}^{2-}$  (**Figure 1**).

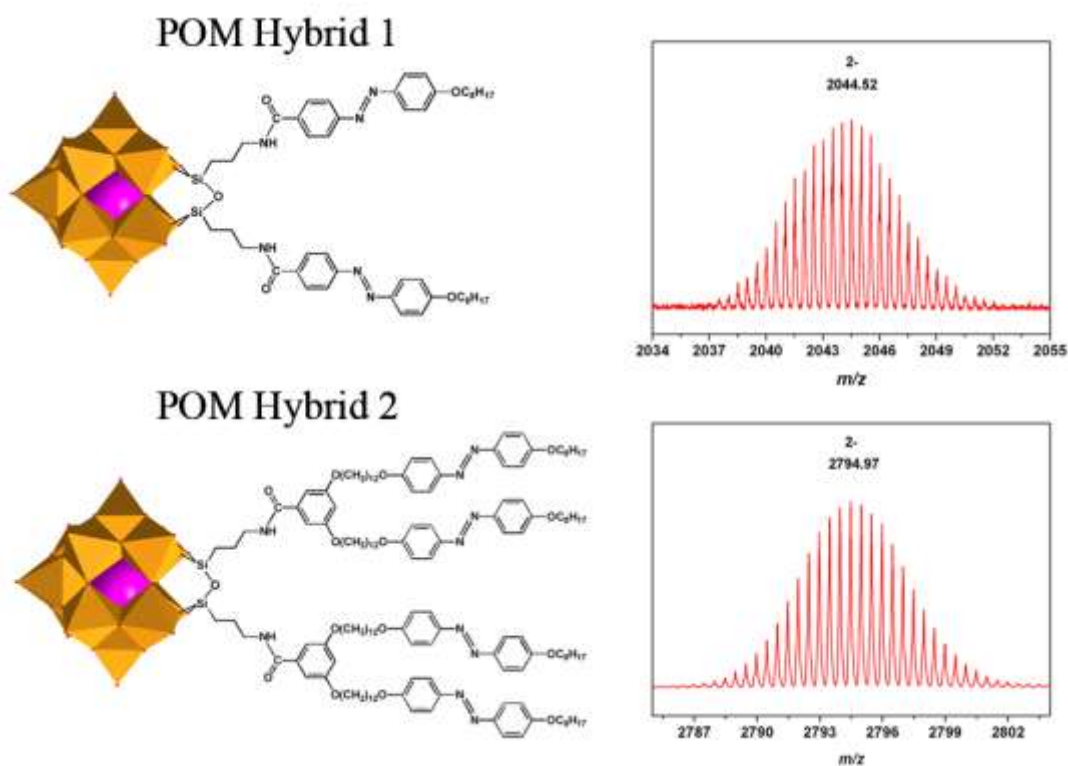


**Fig. 1.** Schematic presentation of POM hybrids and the corresponding ESI-MS spectra



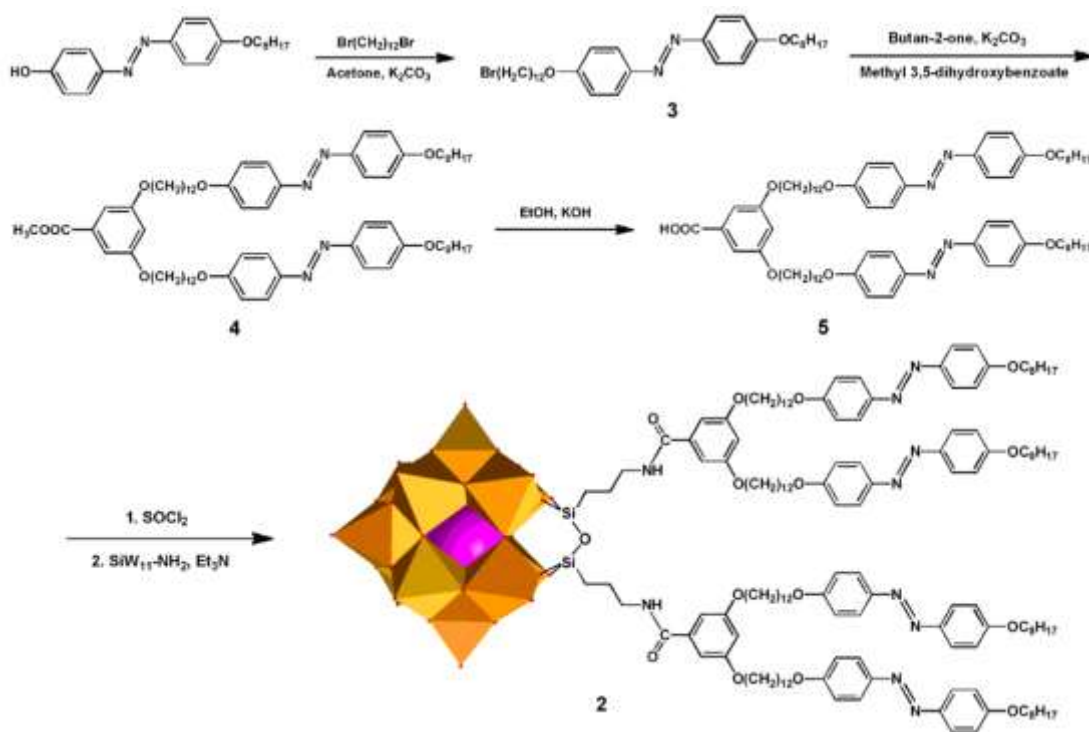


**Fig. 2.** General synthetic procedure of POM Hybrid 2

According to DSC investigation as shown in **Figure S5**, we find that both of these POM hybrids have no LC phases observed on the thermal recycle. Therefore we pay more attention to the molecular structures of POM hybrids that are related to the crucial factors of the stabilization mechanisms of these BP systems as mentioned later, such as biaxiality and elastic constant. **Figure 3** shows the change in UV/Vis spectra of POM Hybrids 1 and 2 under various UV irradiation condition, clearly showing that the *trans* forms of the azobenzene moieties in POM hybrids exhibit absorption maxima at around 350 nm due to a  $\pi\text{-}\pi^*$  transition and at 450 nm due to an  $n\text{-}\pi^*$  transition. Upon UV photoirradiation at 365 nm ( $2\text{ mW}\cdot\text{cm}^{-2}$ ), a distinct decrease in the  $\pi\text{-}\pi^*$  bands and a relatively small amount of increase in the  $n\text{-}\pi^*$  bands are found, which suggests that *trans-cis* photoisomerization of these two POM hybrids takes place upon UV irradiation.

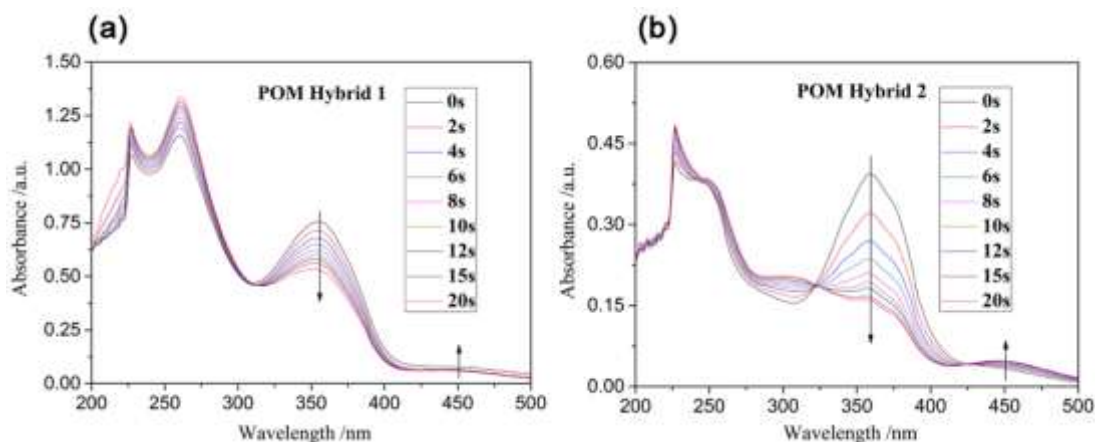


Fig. 3. UV/Vis absorption spectra of (a) POM Hybrid 1 and (b) POM Hybrid 2

under various irradiation conditions

### 3.2. Temperature Ranges of BPs induced by POM hybrids

To evaluate these two POM hybrids on the BP temperature ranges, a series of LC samples doped with different amount of POM hybrids are prepared, and the weight ratios of each component are listed in **Table 1**. In order to avoid a supercooling effect for the misunderstanding of the BPs' stable temperature range, the temperature ranges having a coexistence of BPs (BP I or BP II) and Ch phase or isotropic phase have been excluded from the temperature ranges of BP in this study. Additionally, the Bragg reflection bands in BPs are plotted as a function of temperature to identify different BP phase, such as BP I or BP II. By comparing the temperature ranges of BPs between doped samples with the undoped one, we find that both POM Hybrid 1 and POM Hybrid 2 are beneficial to stabilizing BPs as shown in **Table 1**. For example, by increasing the POM Hybrid from 0 to 3.0 %, the BPs temperature ranges of LC system doped with POM Hybrid 1 increase from 5.9 °C to 20.5 °C in samples A0-A2. By contrast, increase of the POM Hybrid 2 from 0 to 3.0 wt% results in a little increase in the BPs temperature range, i.e., from 5.9

°C to 7.9 °C in samples B0-B2. However, when the concentrations of the POM hybrids are increased from 5.0 wt% to 11.0 wt%, the expansion of BP temperature ranges are inversely suppressed both in the samples of A3-A5 and B3-B5 as shown in **Table 1**, which may be related to the effective solubility of POM hybrids in LC systems.

**Table 1.** Phase transition temperatures and temperature ranges for the LC samples containing POM hybrids

	Mixture ratio of host LC /wt%			Phase transition temperature /°C			Temperature range /°C
	BYLC-X	S811	POM Hybrid 1	BP I	BP II	Iso	$\Delta T$
A0	67	33	-	47.4	52.6	53.3	5.9
A1	67	33	1	40.5	51	51.5	11.0
A2	67	33	3	31.0	--	51.5	20.5
A3	67	33	5	39.7	--	52.0	12.3
A4	67	33	8	42.5	--	52.6	10.1
A5	67	33	11	36.2	--	51.1	14.9
	BYLC-X	S811	POM Hybrid 2	BP I	BP II	Iso	$\Delta T$
B0 (A0)	67	33	-	47.4	52.6	53.3	5.9
B1	67	33	1	--	46.3	52.1	5.8
B2	67	33	3	--	42.0	49.9	7.9
B3	67	33	5	--	40.9	47.7	6.8
B4	67	33	8	--	43.5	49.7	6.2
B5	67	33	11	--	42.5	48.9	6.4

According to the polarized microscope images and temperature dependence of the Bragg reflection from the LC mixtures in **Figure 4**, we surprisingly find that POM Hybrid 1 has a great effect for the stabilization of BP I, while POM Hybrid 2 helps to stabilize BP II. As a representative example, for the sample A2, the polarized microscope texture of BP I are platelet texture with a continuous color change and fine stripes from 51.5 °C to 31 °C as shown in **Figure 4c**, in which no obvious fluctuation of the textures are observed

during the cooling process. Meanwhile, **Figure 4a** illustrates the temperature dependence of the reflection band of the sample A2, it clearly shows that the reflection band of the sample exhibits a continuous change and has a little red shift as the temperature decreases. It is well known that Bragg reflection bands in the temperature regions above and below the transition point are closely bound up with the (100) and (110) reflections of the cubic lattice planes of BP II and BP I, respectively. If the existence of the BP I–BP II transition, the temperature dependence of the Bragg reflection wavelength exhibits a discontinuous change and the wavelength shifts approximately 50-80 nm from BP I to BP II.<sup>4</sup> Therefore, we confirm that there is just BP I in these samples doped with POM Hybrid 1. However, the samples with POM Hybrid 2 exhibit entirely different appearances. Firstly, the featured polarized microscope textures of the sample B3 blended with 5.0 wt% POM hybrid 2 are observed on the cooling process. As shown in **Figure 4d**, the typical texture of BP II appears as similar to that of the previous study.<sup>47</sup> In order to further verify this deduction, we also investigate the temperature dependence of Bragg reflection bands. **Figure 4b** shows the typical temperature dependence of the Bragg reflection band of the sample B3 blended with 5.0 wt% POM Hybrid 2. It is obvious that the Bragg reflection wavelength has a gradual blue-shift as the temperature decreases. This trend corresponds well with that observed for BP II in other case during heating and cooling process, which means that BP II is dominant in this sample.<sup>27</sup> Based on these observation, we therefore confirm that POM Hybrid 2 helps to stabilize BP II.

On the basis of polarized microscope images results and Bragg reflection observations of the samples A0-A5 and B0-B5, two phase diagrams are produced as shown in **Figure 5**. In fact, **Table 1** has already provided information for the phase transition temperatures.

In order to get a direct contrast for the stabilization effect, here we just focus on BP I for A0-A5 and BP II for B0-B5. **Figure 5a** shows the phase diagram for the samples A0-A5 as a function of the POM Hybrid 1 concentration. In the samples A0-A5, the widest temperature range of BP I reaches to  $>20$  °C for the sample A2 during the cooling process. What's more, the lower temperature of BPs is very close to room temperature as shown in **Figure 5a**, which is one of necessary factors of the BPs-LC for display and photonics applications. **Figure 5b** shows the phase diagram for LC samples as a function of the concentration of POM Hybrid 2. For the undoped sample (B0), the temperature range of BP II is around 0.7 °C. Whereas the widest temperature range of BP II for the sample B2 increases to 7.9 °C, which is much wider than that of conventional BP system.

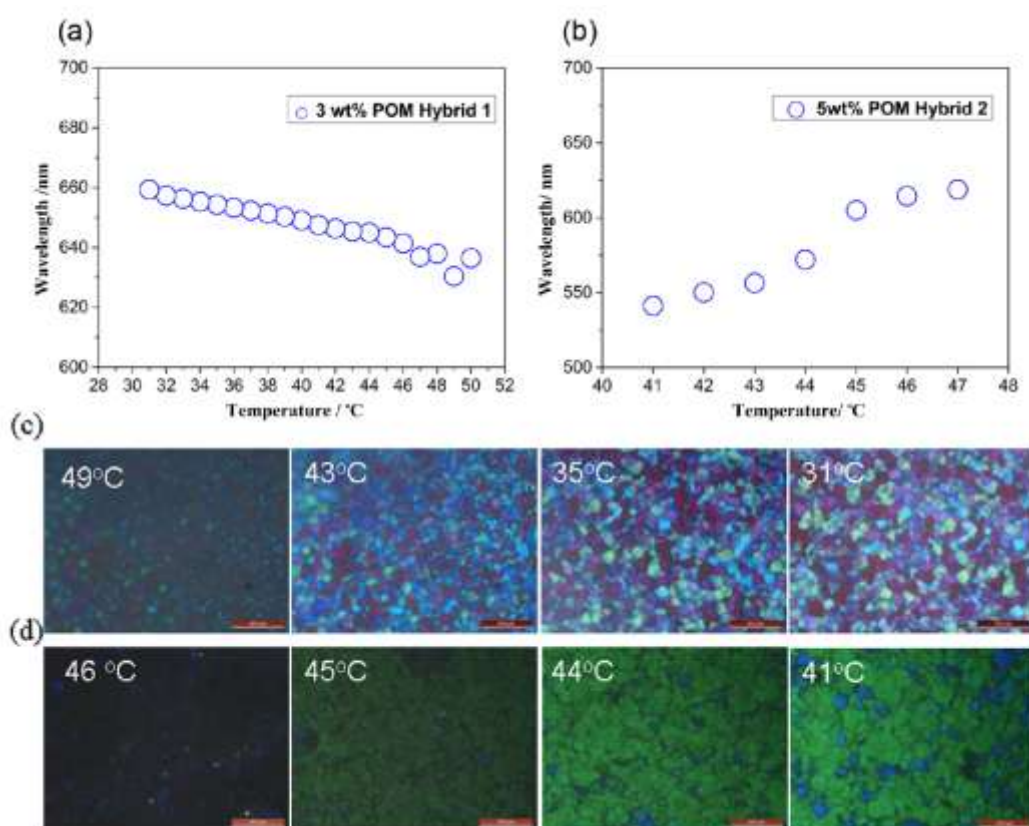


**Fig. 4.** Temperature dependence of the Bragg reflection peak wavelengths for (a) the sample with 3 wt% POM Hybrid 1 and (b) the sample with 5 wt% POM Hybrid 2; (c)

and (d) polarized microscope images of these two samples, respectively.

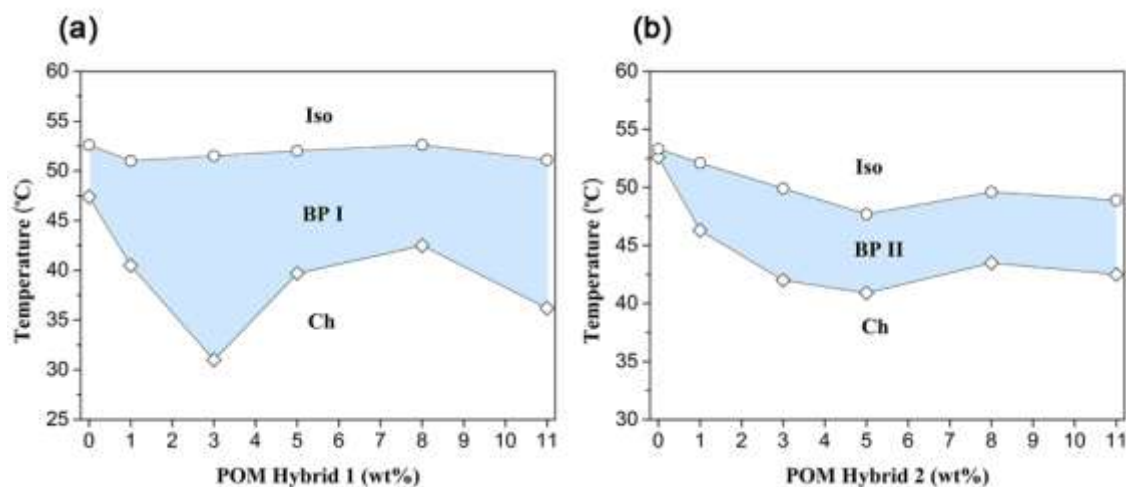


**Fig. 5.** Phase diagram obtained during cooling process for the samples with (a) POM Hybrid 1 and (b) POM Hybrid 2

### 3.3. Mechanisms of POM hybrids for stabilizing the BPs

To get an understanding of how these two POM hybrids affects the BP temperature range of LC systems, we investigated the influence of the doped POM hybrids on the elastic constants of the bulk N-LCs of BYLC-X. Here we prepared the LC samples 1 and 2, in which the weight ratio of POM hybrids is 3.0 % in BYLC-X. In theory, three types of the Frank elastic constants, splay ( $K_{11}$ ), twist ( $K_{22}$ ), and bend ( $K_{33}$ ), have been demonstrated to be closely related with the thermodynamic stability of BPs as mentioned in the previous studies.<sup>14,48,49</sup> The measured and calculated parameters of samples 1 and 2, including  $K_{11}$  and  $K_{33}$ , elastic constant ratio ( $K_{33}/K_{11}$ ), dielectric constant anisotropy ( $\Delta\epsilon$ ), threshold voltage ( $V_{th}$ ), are listed in **Table S3**. Here the temperature dependencies of the elastic constants ( $K_{11}$ ,  $K_{33}$ ) and elastic constant ratio ( $K_{33}/K_{11}$ ) for samples 1 and 2 are shown in **Figure 6**, where  $T$  is the measured temperature and  $T_c$  is the clearing point. It should be noted that  $K_{11}$  and  $K_{33}$  of the samples 1 and 2 are larger than that of the bulk BYLC-X. This may be due to that the existence of counter cations in POM moiety of

POM Hybrids 1 and 2 influences the dielectric performance of the bulk LCs as shown in **Table S3**. Herein,  $K_{11}$  of sample 1 with POM Hybrid 1 is larger than that of sample 2 containing POM Hybrid 2 as shown in **Figure 6a**, whereas  $K_{33}$  of sample 1 is much smaller than that of sample 2 containing POM Hybrid 2 as shown in **Figure 6b**. According to the previous investigations, the smaller  $K_{33}$  should be responsible for the doping-induced enlargement of temperature ranges of thermodynamically stable BPs.<sup>14,25</sup> This may be the reason why the POM Hybrid 1 has a better effect on the stabilization of BPs than POM Hybrid 2 does. Next, the elastic constant ratio ( $K_{33}/K_{11}$ ) of the sample 1 is much smaller than that of sample 2 in **Figure 6c**, but it is very similar to that of the bulk BYLC-X. It has been reported that the elastic constant ratio  $K_{33}/K_{11}$  is relevant to the ratio of molecular length  $L$  to width  $D$  ( $L/D$ ), and the corresponding order parameters of the LC molecules decrease when  $L/D$  ratio of molecules is reduced.<sup>14,25</sup> By comparing the measured  $K_{33}/K_{11}$  of sample 1 with sample 2, it may be reasonable to think that the order parameters of the BYLC-X doped with POM hybrid 1 would be more pronouncedly reduced. As a result, the BPs–Ch transition temperature of the samples doped with POM Hybrid 1 is lower than that of the samples doped with POM hybrid 2 as shown in Table 1. This may be a possible mechanism of stabilization effect of BPs from POM Hybrid 1. Finally, the possible reason why BP II is stable in LC samples with POM Hybrid 2 may be related to the dendritic-like molecular structure of POM Hybrid 2. A similar trend has been found in the dendron-stabilized BPs system, in which the temperature range of BP II was extended to 3.5°C due to the introduction of dendron molecule.<sup>14</sup> Additionally, the higher  $K_{33}$  induced by POM Hybrid 2 may be beneficial to stabilizing BP II as demonstrated in the previous study.<sup>50</sup>

In addition to the above-mentioned factors, as shown in **Figure 1**, bent-like POM Hybrid 1 and dendritic-like POM Hybrid 2 are prepared by covalently grafted azobenzene mesogenic units onto the nanosized POM clusters, and these two rigid wide-body hybrid molecules might have two different axes as demonstrated in the previous studies.<sup>45,46</sup> The molecular biaxiality has been demonstrated to be helpful to induce a biaxial helix that can stabilize DTC structure of the BPs. Therefore, we think the molecular biaxiality in POM hybrids may be another important factor for stabilizing the BPs.<sup>16,18</sup>

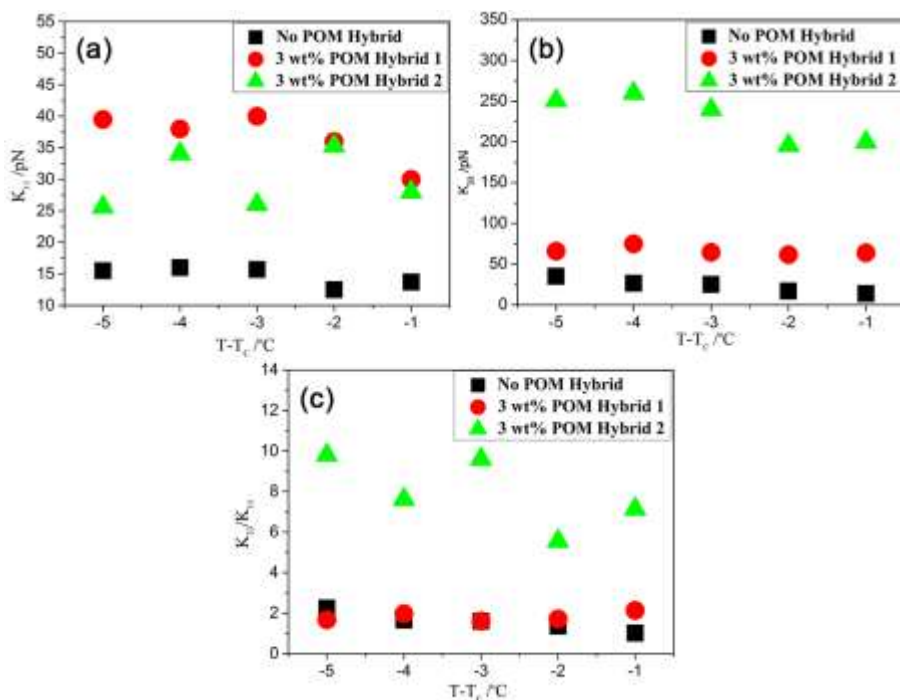


**Fig. 6.** Elastic constants as a function of temperature in Nematic phase: (a) splay elastic constant ( $K_{11}$ ); (b) bend elastic constant ( $K_{33}$ ) and (c) elastic constant ratio ( $K_{33}/K_{11}$ ).  $T$  is the measured temperature and  $T_c$  is the clearing point.

### 3.4. Optical Switching of Bragg Reflection Band of BP II

We then evaluate the effectiveness of the POM hybrid on the optical tuning of reflection band of BP. Different from some previous investigations,<sup>33-35</sup> here we focus on



the optical tuning of BP II, rather than BP I or phase transition from BP I to Ch. Therefore, a LC sample (sample 3) with 36 wt% S811 in 64 wt% BYLC-X doped with 5 wt% POM Hybrid 2 was prepared, in which the temperature ranges of BP II is around 7.5 °C ranged from 48.4 to 40.9 °C on the cooling process. Temperature dependence of the reflection bands of this sample, shown in **Figure 7a** and **7b**, clearly shows that the Bragg reflection band of this sample exhibits a blue shift as the temperature is decreased from the isotropic clearing point. Therefore, we confirm that there is dominant BP II in this sample.

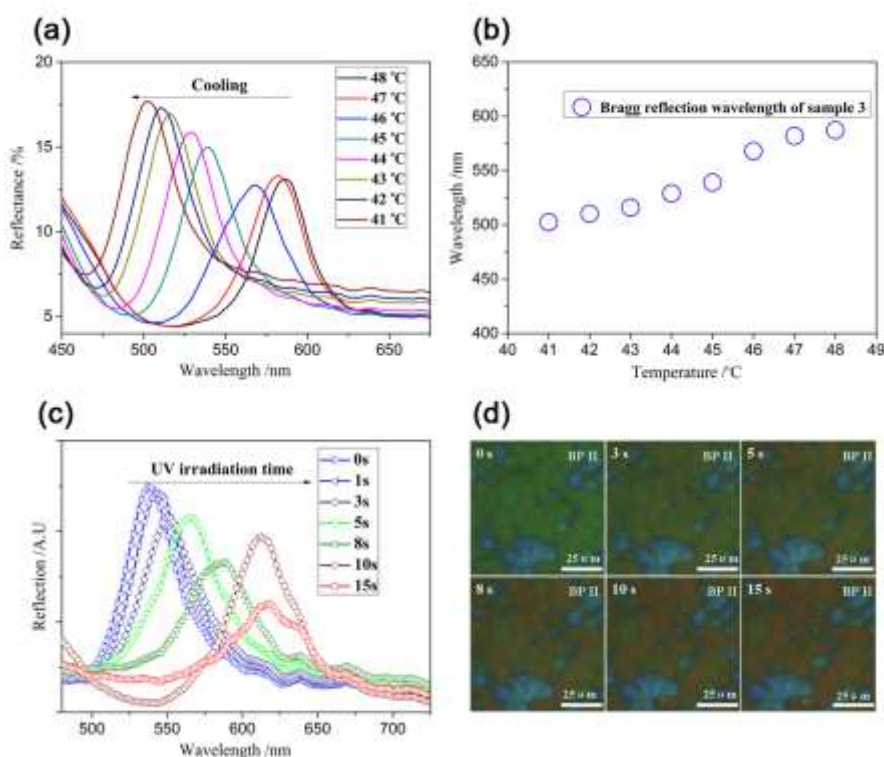


**Fig. 7.** (a) The temperature dependence of the Bragg reflectance wavelength of the sample 3; (b) and the corresponding point plot of Bragg reflection wavelength of the sample 3; (c) the reflectance spectral change of the sample 3 when irradiated by UV light at 45 °C; (d) changes in polarized microscope images of the sample 3 when irradiated by UV light at 45 °C.

We perform the optical switching of BP II of this LC sample doped with POM Hybrid

2 at 45°C. Similarly to the no phase transition from BP II to BP I or Ch on cooling process, a continuous shift of Bragg reflection band is observed at the photo-induced optical behavior of this sample. As shown in **Figure 7c**, the reflection bands has a red-shift from 539 to 617 nm upon UV irradiation (365 nm, 10 mW/cm<sup>2</sup>) and the shift range of Bragg reflection wavelength is 78 nm. After 15s of irradiation, the reflection band of BP II no longer shifts and stays at 617 nm. **Figure 7d** shows the polarized microscope images for the BP II of the sample 3 at 45°C by UV light irradiation. The various BP platelet colors from green to red is observed as the irradiation time increases, which is in agreement with a continuous shift of reflection wavelength under UV irradiation as shown in **Figure 7c**. Additionally, it recovers to the original state when irradiated by visible light (450 nm, 15 mW/cm<sup>2</sup>).

**Figure 8** shows the illustrations of BP-LCs doped with POM Hybrid 2 and the phototuning mechanism of DTC structure in BP II before and after UV light irradiation. It should be noted that this is the first case to effectively tune the Bragg reflection of BP II by UV/Vis light and no phase transitions from BP II to BP I or to Ch are observed. Here the photoresponsive behavior is derived from four azobenzene mesogen groups of POM Hybrid 2, in which azobenzene group has a *trans-cis* isomerization upon UV light irradiation. As demonstrated in **Figure 8**, the UV irradiation causes the bending of the rigid part of the azobenzene moieties in the POM Hybrid 2 resulting from the change of geometrical configuration from *trans-* to *cis-* isomers of azobenzene groups. Here the destabilization effect of *cis*-isomer makes the bulk LC molecules more loose and results in the extension of the DTC structure of BP II for the LC samples doped POM Hybrid 2. Therefore the lattice constants of DTC structure of BP II are increased, leading to the fact

that Bragg reflection band of this sample has a red shift. And the restoration of the reflection will occur when the *cis* isomer turns back to the *trans* form under 450 nm light. We further note that no phase transitions from BP II to BP I or from BP II to Ch happen in this BP system according to our observations of polarized microscopy images in **Figure 7d**, this may be attributed to the fact that the “effect” azobenzene concentration is not enough to change the DTC structure of BP II due to the huge molar mass of the POM moiety, thereby resulting in the optical switching in the range of BP II. Another important reason may be that BP II exhibits higher elastic resistance against lattice deformation by the applied external field compared to BP I due to the existence of cross-linking points of disclination lines in BP II structure.<sup>50</sup>

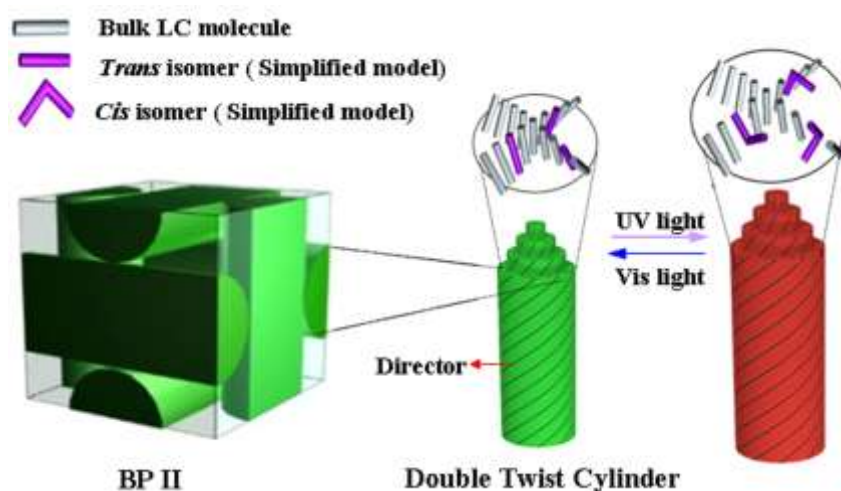


**Fig. 8.** The possible illustration of POM Hybrid 2 doped into the BPs and partial enlargement of DTC structure of BP II before and after irradiation

#### 4. Conclusions

In summary, we have developed two POM-based organic-inorganic hybrids to stabilize blue phases (BPs) and addressed the stabilization mechanism. Both these two POMs

organic-inorganic hybrids are conducive to stabilizing BPs, bent-like POM Hybrid 1 has a positive effect on the stabilization of the BP I, while dendritic-like POMs Hybrid 2 could help to stabilize BP II. The related mechanism may be caused by the difference of elastic properties and orientational order of LC molecules induced by POM hybrids. Additionally, the optically switching of Bragg reflection wavelength of BP II based on dendritic-like POM Hybrid 2 has been achieved. Our molecular design of organic-inorganic hybrids gives rise to a new strategy for both the stabilization of BPs and optical switching of Bragg reflection of BPs.

**Acknowledgements:**

This research was supported by National Natural Science foundation (Grant No. 51373013, 21222104), Beijing Young Talents Plan (YETP0489), the Fundamental Research Funds for the Central Universities (RC1302, YS1406) and Beijing Engineering Center for Hierarchical Catalysts.

**References:**

- 1 I.-C. Khoo, *Liquid Crystals*, 2nd ed. John Wiley & Sons, Inc., Hoboken, New Jersey, 2007, 1-22.
- 2 P.G. De Gennes, J. Prost, *The physics of liquid crystals*, Oxford University Press, New York, 1993.
- 3 W. Cao, A. Munoz, P. Palfy-Muhoray and B. Taheri, *Nat. Mater.*, 2002, **1**, 111-113.
- 4 H. J. Coles and M. N. Pivnenko, *Nature*, 2005, **436**, 997-1000.
- 5 F. Castles, F. V. Day, S. M. Morris, D. H. Ko, D. J. Gardiner, M. M. Qasim, S. Nosheen, P. J. W. Hands, S. S. Choi, R. H. Friend and H. J. Coles, *Nat. Mater.*, 2012, **11**, 599-603.
- 6 O. D. Lavrentovich, *Proc. Natl. Acad. Sci.*, 2011, **108**, 5143-5144.
- 7 A. Yoshizawa, *RSC Adv.*, 2013, **3**, 25475-25497.
- 8 P. P. Crooker, in *Chirality in Liquid Crystals*, ed. H.-S. Kitzerow and C. Bahr, Springer, New York, 2001, pp. 186-222.
- 9 D. C. Wright and N. D. Mermin, *Rev. Mod. Phys.*, 1989, **61**, 385-432.
- 10 K. Higashiguchi, K. Yasui and H. Kikuchi, *J. Am. Chem. Soc.*, 2008, **130**, 6326-6327.
- 11 O. Henrich, K. Stratford, M. E. Cates and D. Marenduzzo, *Phys. Rev. Lett.*, 2011, **106**, 107801.
- 12 H. Kikuchi, M. Yokota, Y. Hisakado, H. Yang and T. Kajiyama, *Nat. Mater.*, 2002, **1**, 64-68.
- 13 W. He, G. Pan, Z. Yang, D. Zhao, G. Niu, W. Huang, X. Yuan, J. Guo, H. Cao and H. Yang, *Adv. Mater.*, 2009, **21**, 2050-2053.
- 14 S. Shibayama, H. Higuchi, Y. Okumura and H. Kikuchi, *Adv. Funct. Mater.*, 2013, **23**, 2387-2396.

- 15 I. Dierking, W. Blenkhorn, E. Credland, W. Drake, R. Kociuruba, B. Kayser and T. Michael, *Soft Matter*, 2012, **8**, 4355-4362.
- 16 Y. Shi, X. W. Wang, J. Wei, H. Yang and J. B. Guo, *Soft Matter*, 2013, **9**, 10186-10195.
- 17 J. B. Guo, Y. Shi, X. Han, O. Y. Jin, J. Wei and H. Yang, *J. Mater. Chem. C*, 2013, **1**, 947-957.
- 18 L. Wang, W. He, X. Xiao, Q. Yang, B. Li, P. Yang and H. Yang, *J. Mater. Chem.*, 2012, **22**, 2383-2386.
- 19 L. Wang, W. He, X. Xiao, M. Wang, M. Wang, P. Yang, Z. Zhou, H. Yang, H. Yu and Y. Lu, *J. Mater. Chem.*, 2012, **22**, 19629-19633.
- 20 X. Chen, L. Wang, C. Li, J. Xiao, H. Ding, X. Liu, X. Zhang, W. He and H. Yang, *Chem. Commun.*, 2013, **49**, 10097-10099.
- 21 H. Yoshida, Y. Tanaka, K. Kawamoto, H. Kubo, T. Tsuda, A. Fujii, S. Kuwabata, H. Kikuchi and M. Ozaki, *Appl. Phys. Express*, 2009, **2**, 121501.
- 22 E. Karatairi, B. Rozic, Z. Kutnjak, V. Tzitzios, G. Nounesis, G. Cordoyiannis, J. Thoen, C. Glorieux and S. Kralj, *Phys. Rev. E*, 2010, **81**, 041703.
- 23 L. Wang, W. He, X. Xiao, F. Meng, Y. Zhang, P. Yang, L. Wang, J. Mei, H. Yang and Y. Lu, *Small*, 2012, **8**, 2189-2193.
- 24 J. M. Wong, J. Y. Hwang and L. C. Chien, *Soft Matter*, 2011, **7**, 7956-7959.
- 25 K. Kakisaka, H. Higuchi, Y. Okumura and H. Kikuchi, *J. Mater. Chem. C*, 2014, **2**, 6467-6470.
- 26 C.-L. Wei, T.-C. Chen, P. Raghunath, M.-C. Lin and H.-C. Lin, *RSC Adv.*, 2015, **5**, 4615-4622.

27. K.-W. Park, M.-J. Gim, S. Kim, S.-T. Hur and S.-W. Choi, *ACS Appl. Mater. Interfaces*, 2013, **5**, 8025-8029.
- 28 K. Kishikawa, T. Sugiyama, T. Watanabe, S. Aoyagi, M. Kohri, T. Taniguchi, M. Takahashi and S. Kohmoto, *J. Phys. Chem. B*, 2014, **118**, 10319-10332.
- 29 A. Yoshizawa, M. Sato and J. Rokunohe, *J. Mater. Chem.*, 2005, **15**, 3285-3290.
- 30 C. V. Yelamaggad, I. S. Shashikala, G. Liao, D. S. S. Rao, S. K. Prasad, Q. Li and A. Jakli, *Chem. Mater.*, 2006, **18**, 6100-6102.
- 31 A. Yoshizawa, Y. Kogawa, K. Kobayashi, Y. Takanishi and J. Yamamoto, *J. Mater. Chem.*, 2009, **19**, 5759-5764.
- 32 S. Taushanoff, K. V. Le, J. Williams, R. J. Twieg, B. K. Sadashiva, H. Takezoe and A. Jakli, *J. Mater. Chem.*, 2010, **20**, 5893-5898.
- 33 J. B. Guo, J. Wang, J. Y. Zhang, Y. Shi, X. W. Wang and J. Wei, *J. Mater. Chem. C*, 2014, **2**, 9159-9166.
- 34 O. Y. Jin, D. W. Fu, J. Wei, H. Yang and J. B. Guo, *RSC Adv.*, 2014, **4**, 28597-28600.
- 35 T. H. Lin , Y. Li , C. T. Wang , H. C. Jau , C. W. Chen, C. C. Li , H. K. Bisoyi , T. J. Bunning and Q. Li, *Adv Mater.*, 2013, **25**, 5050-5054.
- 36 L. Cronin and A. Müller, *Chem. Soc. Rev.*, 2012, **41**, 7325-7648.
- 37 Y.-F. Song and R. Tsunashima, *Chem. Soc. Rev.*, 2012, **41**, 7384–7402.
- 38 D.-L. Long, R. Tsunashima and L. Cronin, *Angew. Chem. Int. Ed.*, 2010, **49**, 1736-1758.
- 39 B. Rausch, M. D. Symes, G. Chisholm and L. Cronin, *Science*, 2014, **345**, 1326-1330.
- 40 C. Busche, L. Vilà-Nadal, J. Yan, H. N. Miras, D.-L. Long, V. P. Georgiev, A. Asenoc, R. H. Pedersen, N. Gadegaard, M. M. Mirza, D. J. Paul, J. M. Poblet and L. Cronin,

- Nature*, 2014, **515**, 545-549.
- 41 S.-T. Zheng and G.-Y. Yang, *Chem. Soc. Rev.*, 2012, **41**, 7623-7646.
- 42 L. Wei, Q. Wei, Z.-E. Lin, Q. Meng, H. He, B.-F. Yang, and G.-Y. Yang, *Angew. Chem. Int. Ed.*, 2014, **53**, 7188-7191.
- 43 S. Herrmann, M. Kostrzewa, A. Wierschem and C. Streb, *Angew. Chem. Int. Ed.*, 2014, **53**, 13596-13599.
- 44 S. Landsmann, M. Wessig, M. Schmid, H. Cölfen and S. Polarz, *Angew. Chem. Int. Ed.*, 2012, **51**, 5995-5999.
- 45 C.-G. Lin, W. Chen, S. Omwoma and Y.-F. Song, *J. Mater. Chem. C*, 2015, **3**, 15-18.
- 46 W. Chen, D. Ma, J. Yan, T. Boyd, L. Cronin, D.-L. Long and Y.-F. Song, *ChemPlusChem.*, 2013, **78**, 1226-1229.
- 47 C.-C. Huang, C.-C. Hsu, L.-W. Chen and Y.-L. Cheng, *Soft Matter*, 2014, **10**, 9343-9351.
- 48 H. Chen, H. Liu, J. Lai, C. Chiu and J. Chou, *Appl. Phys. Lett.*, 2010, **97**, 181919.
- 49 S. T. Hur, M. J. Gim, H. J. Yoo, S. W. Choi and H. Takezoe, *Soft Matter*, 2011, **7**, 8800-8803.
- 50 H. Choi, H. Higuchi and H. Kikuchi, *Appl. Phys. Lett.*, 2011, **98**, 131905.



Graphic Abstract:

## Table of contents entry

**Text:**

Two polyoxometalate-based organic-inorganic hybrids have been demonstrated to be capable of stabilizing and optically switching of liquid crystal blue phase.

**Color graphic:**

